



Direct detection experiments and dark energy

Luca Visinelli

Frascati National Laboratories

INFN Fellini fellow

Marie Skłodowska-Curie Grant no.754496

Based on: 2103.15834, 1911.12374

XENONIT and new physics



Excess electronic recoil events in XENON1T

XENON Collaboration • E. Aprile (Columbia U.) [Show All\(139\)](#)

Jun 17, 2020

We report results from searches for new physics with low-energy electronic recoil data recorded with the XENON1T detector. With an exposure of 0.65 tonne-years and an unprecedentedly low background rate of $76 \pm 2_{\text{stat}}$ events/(tonne \times year \times keV) between 1 and 30 keV, the data enable one of the most sensitive searches for solar axions, an enhanced neutrino magnetic moment using solar neutrinos, and bosonic dark matter. An excess over known backgrounds is observed at low energies and most prominent between 2 and 3 keV. The solar axion model has a 3.4σ significance, and a three-dimensional 90% confidence surface is reported for axion couplings to electrons, photons, and nucleons. This surface is inscribed in the cuboid defined by $g_{ae} < 3.8 \times 10^{-12}$, $g_{a\text{neff}} < 4.8 \times 10^{-18}$, and $g_{a\gamma} < 7.7 \times 10^{-22} \text{ GeV}^{-1}$, and excludes either $g_{ae} = 0$ or $g_{a\gamma} = g_{a\text{neff}} = 0$. The neutrino magnetic moment signal is similarly favored over background at 3.2σ , and a confidence interval of $\mu_{\nu} \in (1.4, 2.9) \times 10^{-11} \mu\text{B}$ (90% C.L.) is reported. Both results are in strong tension with stellar constraints. The excess can also be explained by β decays of tritium at 3.2σ significance with a corresponding tritium concentration in xenon of $(6.2 \pm 2.0) \times 10^{-25} \text{ mol/mol}$. Such a trace amount can neither be confirmed nor excluded with current knowledge of its production and reduction mechanisms. The significances of the solar axion and neutrino magnetic moment hypotheses are decreased to 2.0σ and 0.9σ , respectively, if an unconstrained tritium component is included in the fitting. With respect to bosonic dark matter, the excess favors a monoenergetic peak at $(2.3 \pm 0.2) \text{ keV}$ (68% C.L.) with a 3.0σ global (4.0σ local) significance over background. This analysis sets the most restrictive direct constraints to date on pseudoscalar and vector bosonic dark matter for most masses between 1 and 210 keV/c². We also consider the possibility that Ar37 may be present in the detector, yielding a 2.82 keV peak from electron capture. Contrary to tritium, the Ar37 concentration can be tightly constrained and is found to be negligible.

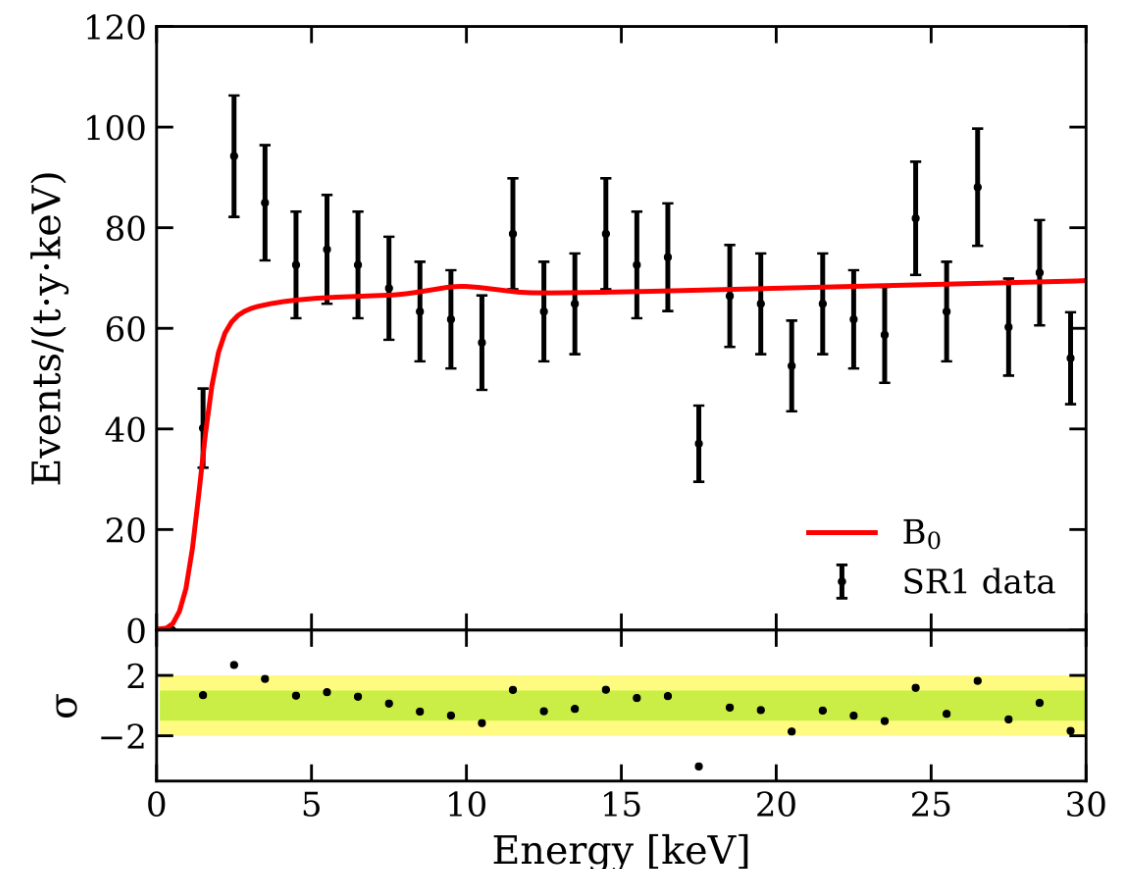
26 pages

Published in: *Phys.Rev.D* 102 (2020) 7, 072004

e-Print: [2006.09721](#) [hep-ex]

DOI: [10.1103/PhysRevD.102.072004](#)

Experiments: XENON1T



Signal is smeared with a Gaussian of width

$$\sigma(E) = a \cdot \sqrt{E} + b \cdot E, \quad (1)$$

with $a = (0.310 \pm 0.004) \sqrt{\text{keV}}$ and $b = 0.0037 \pm 0.0003$.

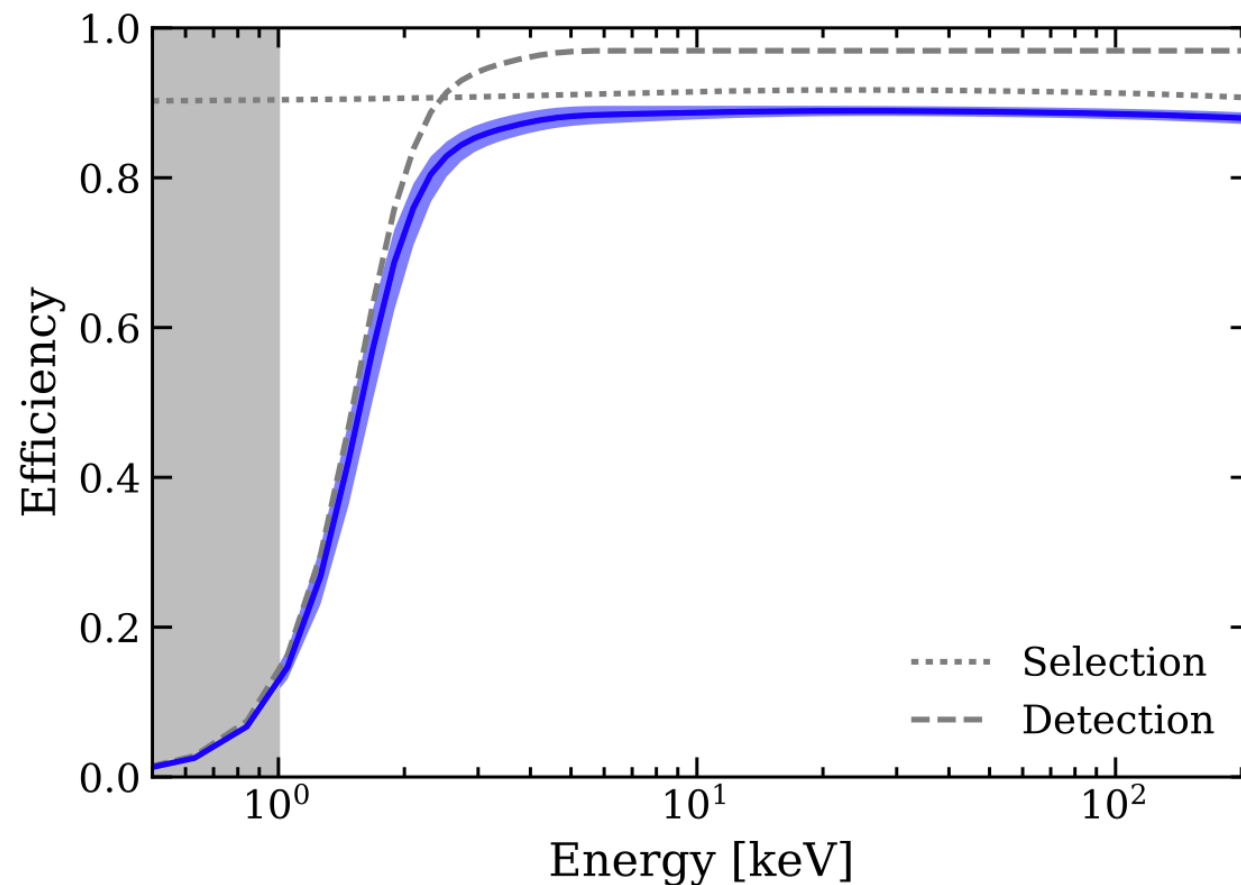


FIG. 2. Efficiency as a function of energy. The dashed (dotted) line refers to detection (selection) efficiency, while the blue curve and band illustrate the total efficiency and the associated 1- σ uncertainty, respectively. The detection threshold is indicated by the right bound of the gray shaded region.

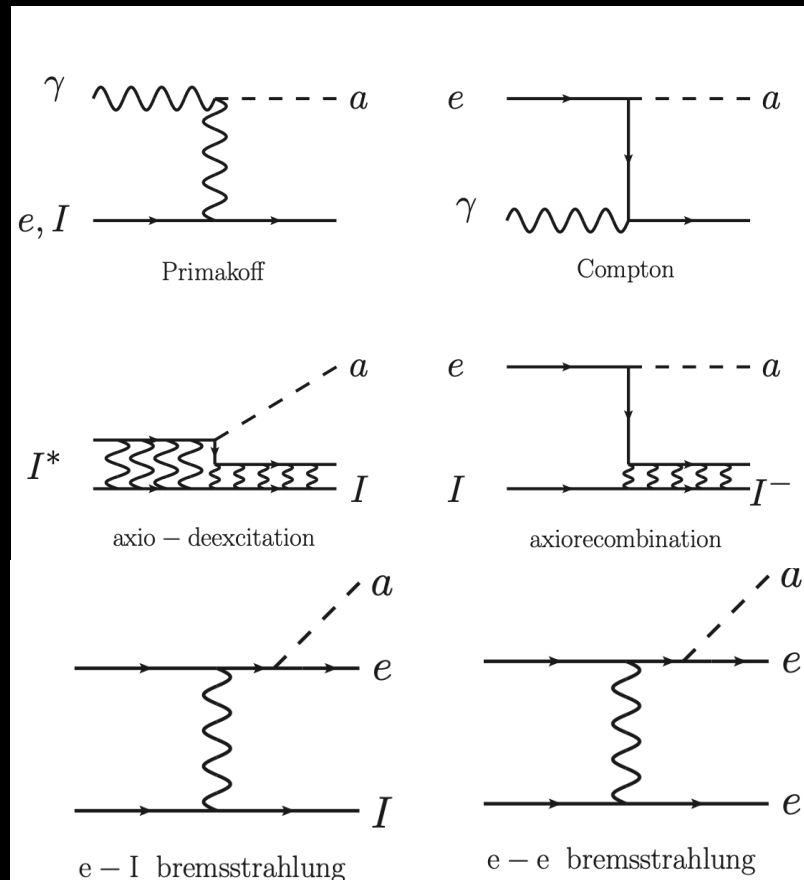
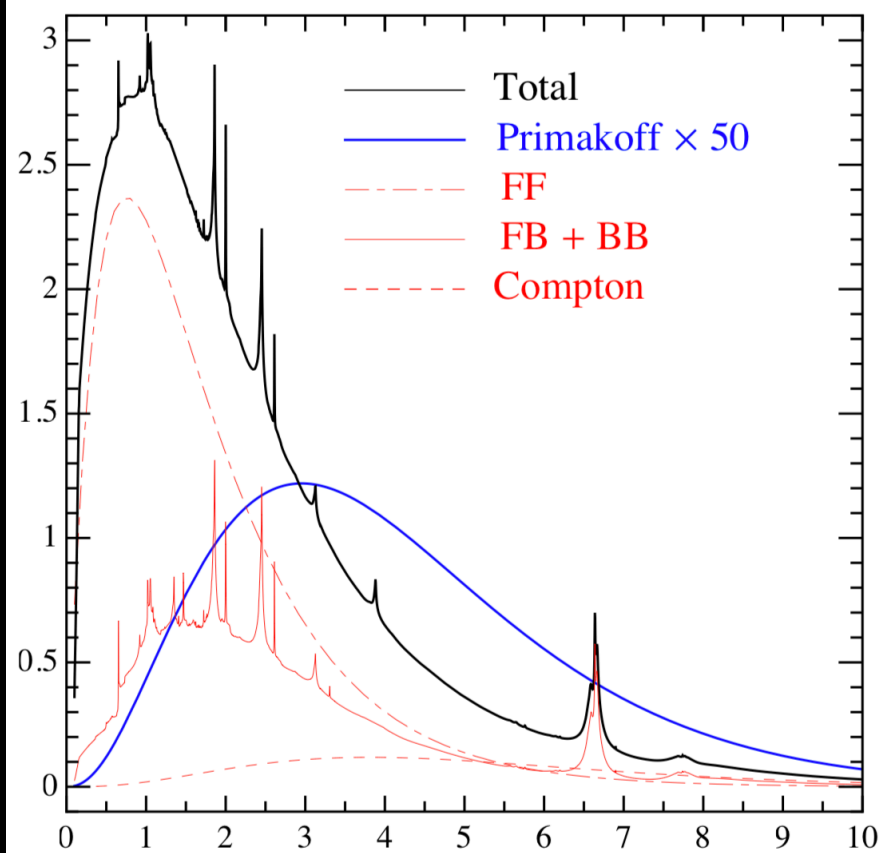
$$\mathcal{L}_{\text{int}} = \frac{1}{4} g_{a\gamma} a F_{\mu\nu} \tilde{F}^{\mu\nu} + g_{ae} \frac{\partial_\mu a}{2m_e} \bar{e} \gamma^\mu \gamma_5 e,$$

Solar axion flux from the axion–electron coupling

Javier Redondo

In non-hadronic axion models, where axions couple to electrons at tree level, the solar axion flux is completely dominated by the ABC reactions (Atomic recombination and deexcitation, Bremsstrahlung and Compton). In this paper the ABC flux is computed from available libraries of monochromatic photon radiative opacities (OP, LEDCOP and OPAS) by exploiting the relations between axion and photon emission cross sections. These results turn to be $\sim 30\%$ larger than previous estimates due to atomic recombination (free-bound electron transitions) and deexcitation (bound-bound), which were not previously taken into account.

ABC (g_{ae}) + Primakoff ($g_{a\gamma}$)

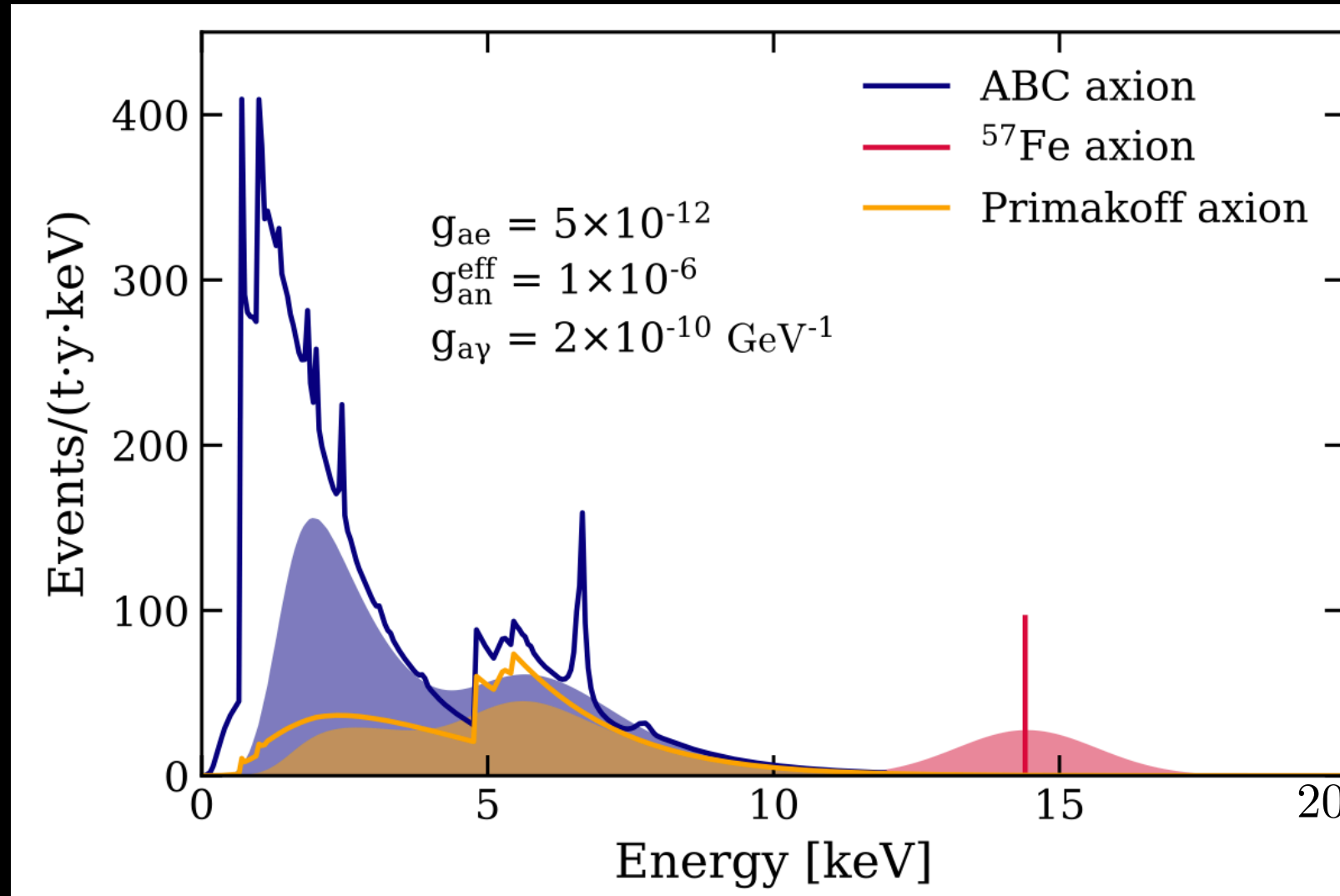


$$\frac{d\Phi_a^{\text{Prim}}}{dE_a} = \left(\frac{g_{a\gamma}}{\text{GeV}^{-1}} \right)^2 \left(\frac{E_a}{\text{keV}} \right)^{2.481} e^{-E_a/(1.205 \text{ keV})} \times 6 \times 10^{30} \text{ cm}^{-2} \text{ s}^{-1} \text{ keV}^{-1},$$

$$\Phi_a^{\text{ABC}} \propto g_{ae}^2$$

+ Iron transition line

$$\Phi_a^{57\text{Fe}} = \left(\frac{k_a}{k_\gamma} \right)^3 \times 4.56 \times 10^{23} (g_{\text{an}}^{\text{eff}})^2 \text{ cm}^{-2} \text{ s}^{-1},$$



DFSZ models: axion couples at tree level to electron (ABC dominates)

KSVZ models: axion couples to electrons through loops (Primakoff dominates)

Bosonic dark matter

Assume DM is an axion-like particle (ALP) in the keV mass range

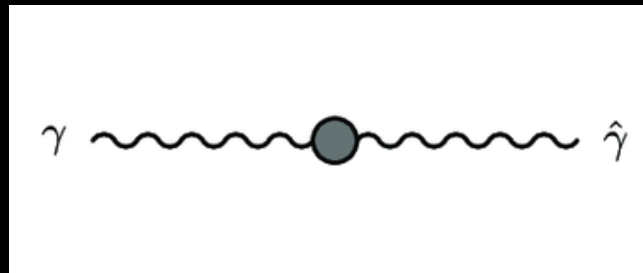
This particle is not the QCD axion that can solve the strong-CP problem!

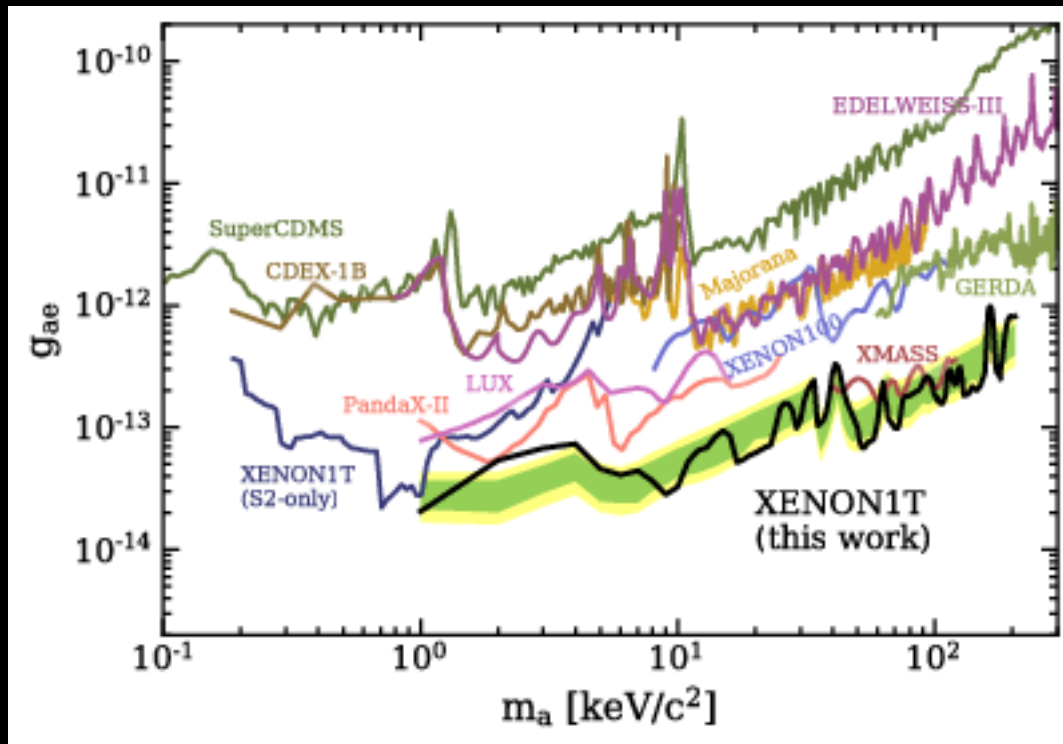
$$R \simeq \frac{1.5 \times 10^{19}}{A} g_{ae}^2 \left(\frac{m_a}{\text{keV}/c^2} \right) \left(\frac{\sigma_{pe}}{b} \right) \text{kg}^{-1} \text{d}^{-1}$$

Assume DM is a vector-like particle in the keV mass range

$$R \simeq \frac{4.7 \times 10^{23}}{A} \kappa^2 \left(\frac{\text{keV}/c^2}{m_V} \right) \left(\frac{\sigma_{pe}}{b} \right) \text{kg}^{-1} \text{d}^{-1}$$

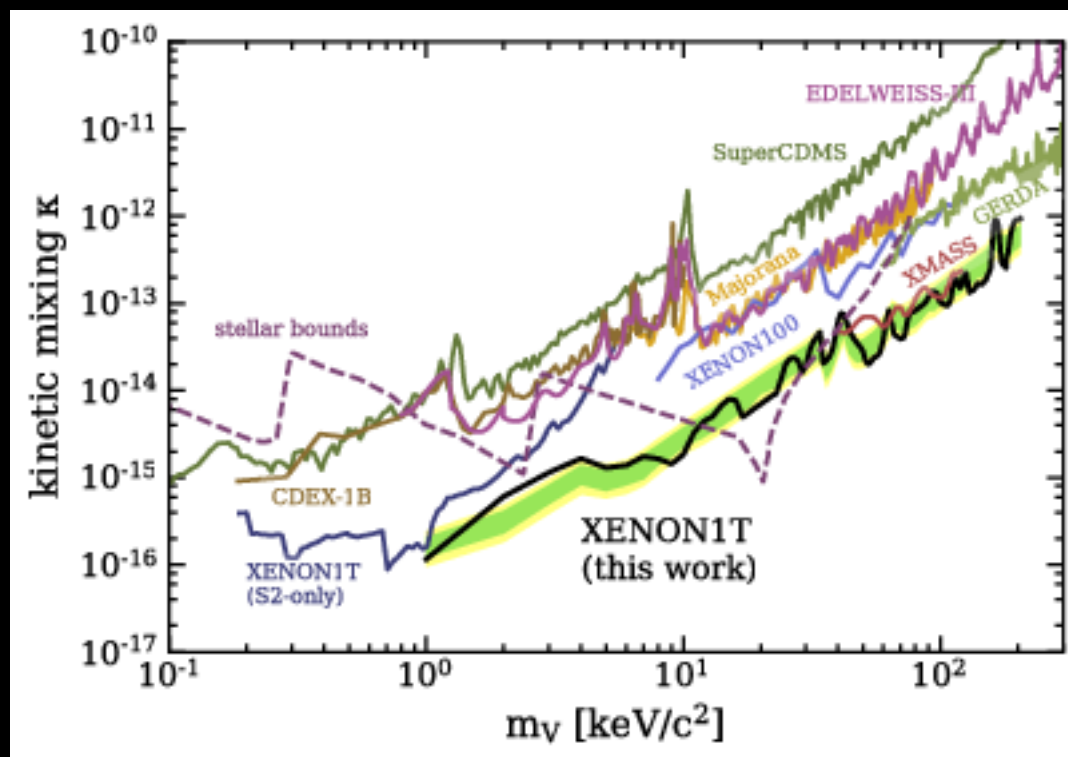
κ parametrizes the mixing between the photon and the dark photon





Constraints on couplings for ALP (top) and vector (bottom) DM

The XENON1T limits (90% C.L.) are shown in black with the expected $1(2)\sigma$ sensitivities in green (yellow)



Limits from other detectors or astrophysical constraints are also shown for both the pseudoscalar and vector cases

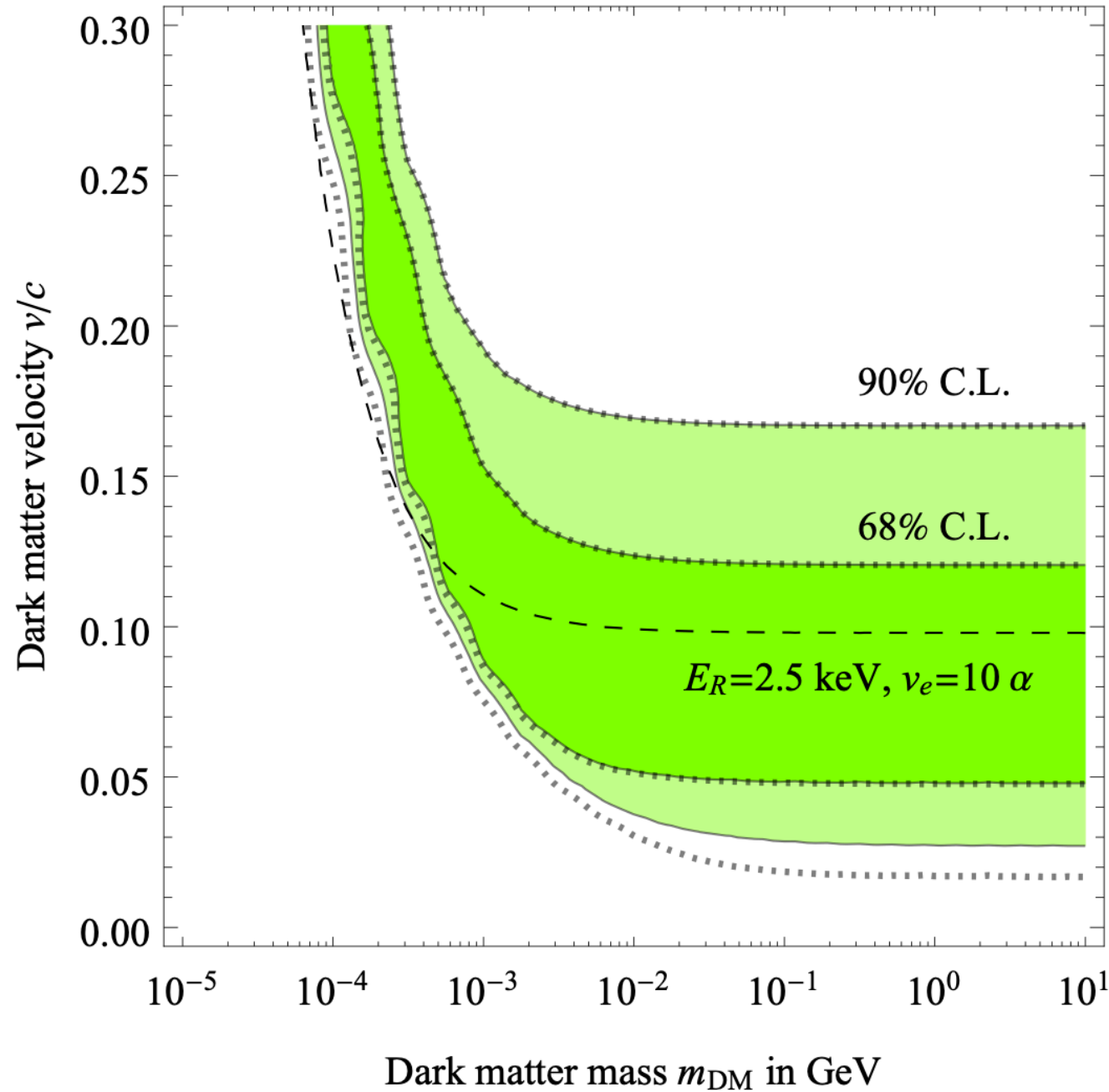


FIG. 2. *Fit to the XENON1T excess as a function of the DM mass and velocity assuming negligible tritium (continuous contours) and allowing for a free tritium abundance (dotted contours). The numerical fit roughly follows the analytic estimate of eq. (1) (dashed curve).*

For a fixed DM velocity v_{DM} (hereafter denoted by v to simplify the notation), the differential cross-section is

$$\frac{d\sigma v}{dE_R} = \frac{\sigma_e}{2m_e v} \int_{q_-}^{q_+} a_0^2 q dq |F(q)|^2 K(E_R, q), \quad (3)$$

where σ_e is the free electron cross-section at fixed momentum transfer $q = 1/a_0$, where $a_0 = 1/(\alpha m_e)$ is the Bohr radius. The limits of integration are

$$q_{\pm} = m_{\text{DM}} v \pm \sqrt{m_{\text{DM}}^2 v^2 - 2m_{\text{DM}} E_R}. \quad (4)$$

We assume the DM form factor $F(q) = 1$ obtained,

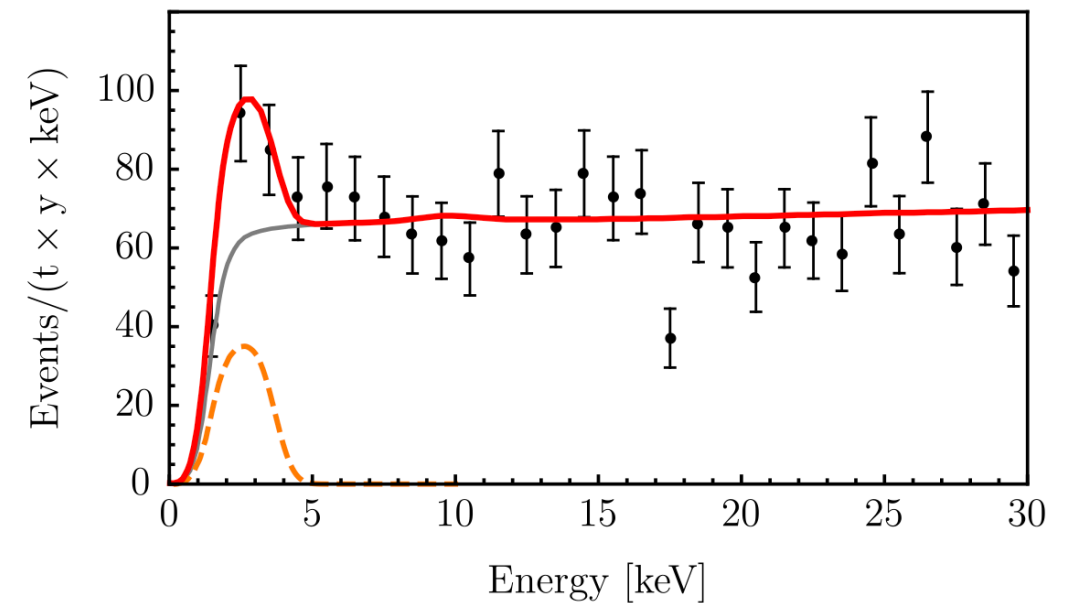


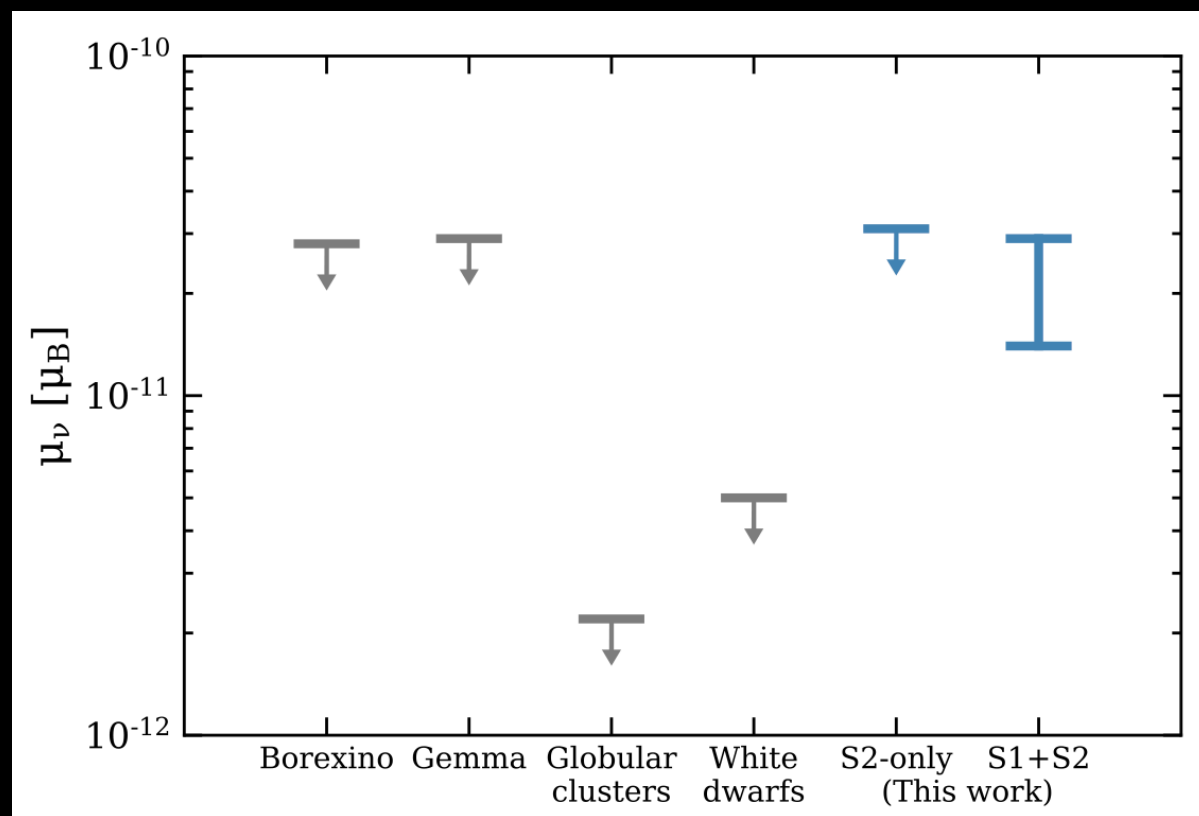
FIG. 1: *The energy spectrum of electrons for a benchmark with $m_{\text{BDM}} = 10$ GeV, $v_{\text{BDM}} = 0.06 c$, $\sigma_{\text{elec}} = 4 \times 10^{-29} \text{ cm}^2$ and BDM flux $\Phi^{\text{BDM}} = 10^{-6} \text{ cm}^{-2} \text{ s}^{-1}$. The dashed orange line represents the contribution from BDM-electron scattering after including the energy resolution and detection efficiency. The red line shows the total electron energy distribution at XENON1T.*

We expect $\mu_\nu \sim 10^{-20} \mu_B$ for massive SM neutrinos

$\mu_\nu < 2.8 \times 10^{-11} \mu_B$ from Borexino

If $\mu_\nu \gtrsim 10^{-15} \mu_B$ then neutrinos are Majorana

$$\frac{d\sigma_\mu}{dE_r} = \mu_\nu^2 \alpha \left(\frac{1}{E_r} - \frac{1}{E_\nu} \right)$$



The 90% confidence interval for μ_ν from this analysis is given by

$$\mu_\nu \in (1.4, 2.9) \times 10^{-11} \mu_B,$$

How can we detect dark energy?

To date, very little is known about DE (compared to DM)

A cosmological constant Λ could serve as DE if

$$\Lambda \sim (H_0 M_{\text{Pl}})^2 \sim (\text{meV})^4$$

However, theory expects a much larger value $\Lambda \sim M_{\text{Pl}}^4$

A scalar field ϕ of mass m_ϕ would also behave as DE today if

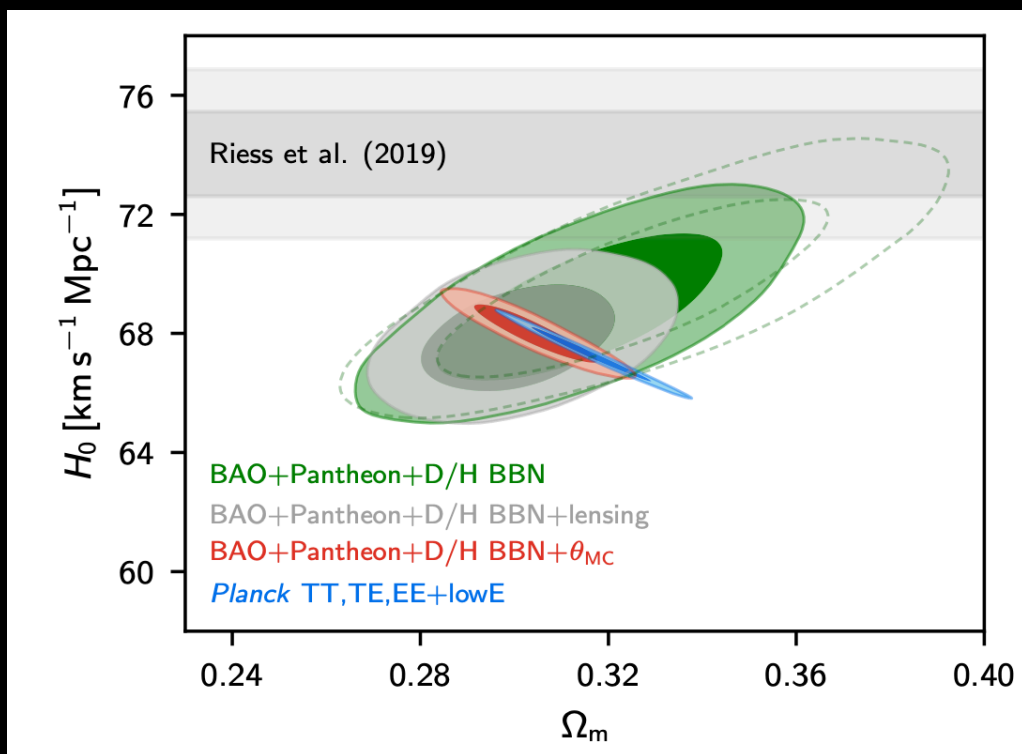
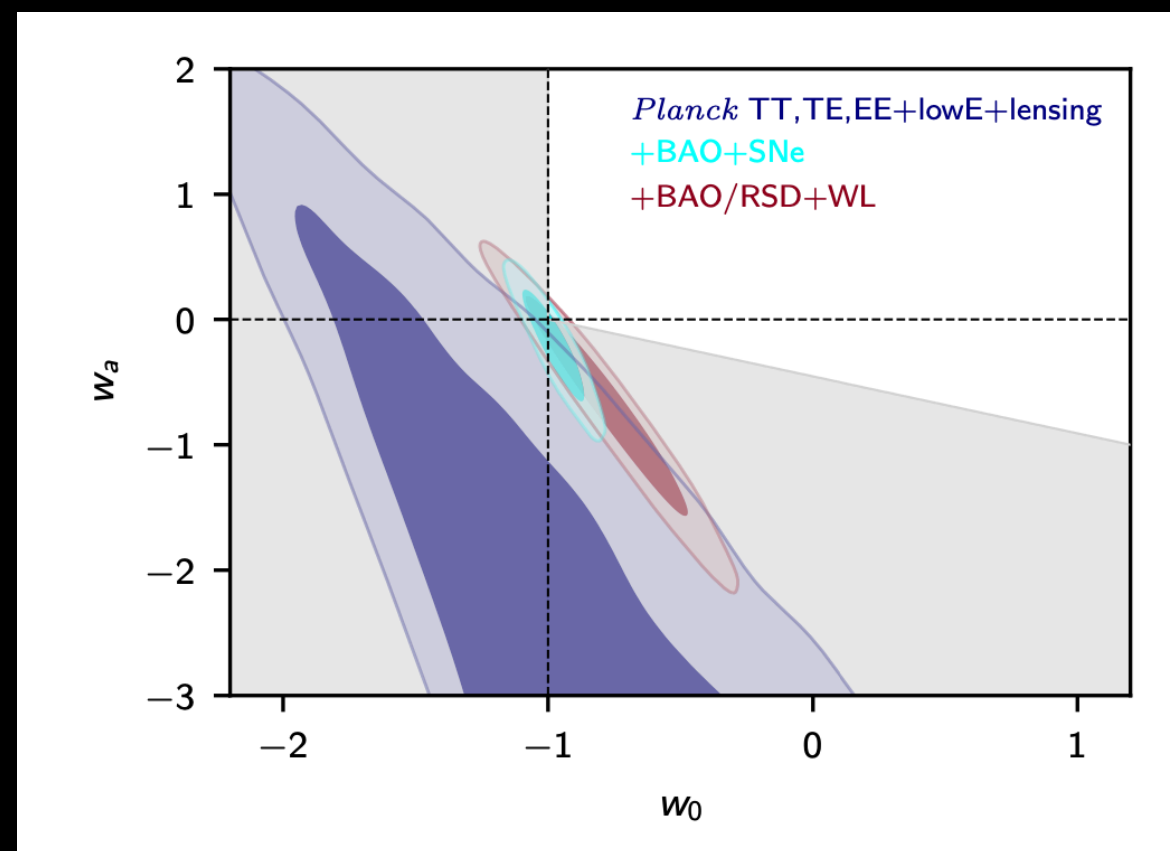
$$m_\phi \lesssim H_0 \sim 10^{-33} \text{ eV} \quad (\text{see e.g. LV\&Vagnozzi 19})$$

The picture is not as simple as expected

e.g. DE model with e.o.s.

$$w(a) = w_0 + w_a(1 - a)$$

Data do not favor a CC



Mismatch between the H_0 coming from early- and late-time measurements

(Planck18)

Baryon - dark energy scattering

A scattering term between baryon and DE is allowed in cosmology

Monthly Notices
of the
ROYAL ASTRONOMICAL SOCIETY

MNRAS **493**, 1139–1152 (2020)
Advance Access publication 2020 February 3

doi:10.1093/mnras/staa311

Do we have any hope of detecting scattering between dark energy and baryons through cosmology?

Sunny Vagnozzi ¹  ¹   Luca Visinelli, ² Olga Mena ³ and David F. Mota ⁴

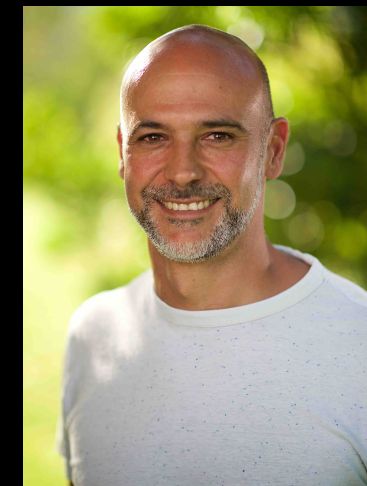
¹*Kavli Institute for Cosmology, University of Cambridge, Madingley Road, Cambridge CB3 0HA, UK*
²*Gravitation Astroparticle Physics Amsterdam (GRAPPA), University of Amsterdam, Science Park 904, NL-1098 XH Amsterdam, the Netherlands*
³*Instituto de Física Corpuscular (IFIC), University of Valencia-CSIC, E-46980 Valencia, Spain*
⁴*Institute of Theoretical Astrophysics, University of Oslo, P.O. Box 1029 Blindern, N-0315 Oslo, Norway*



Sunny Vagnozzi



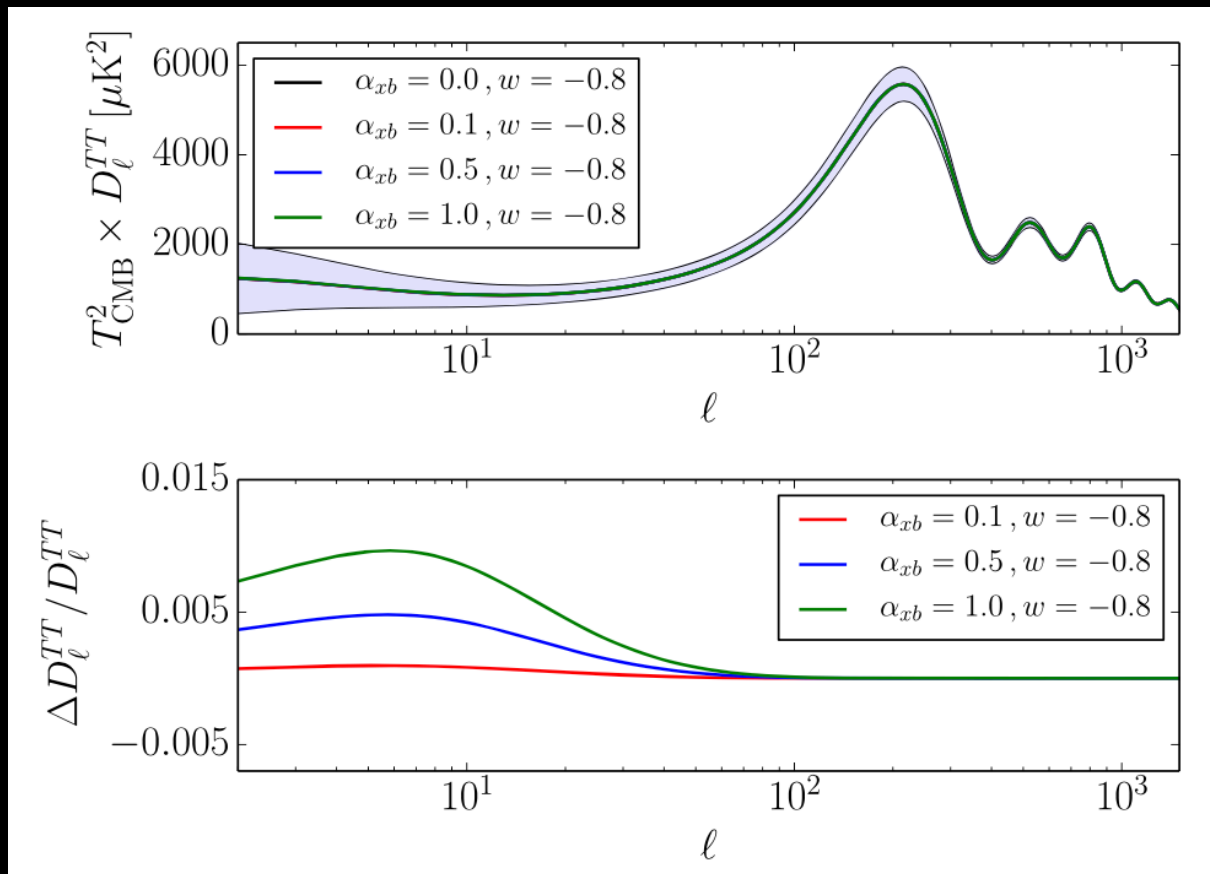
Olga Mena



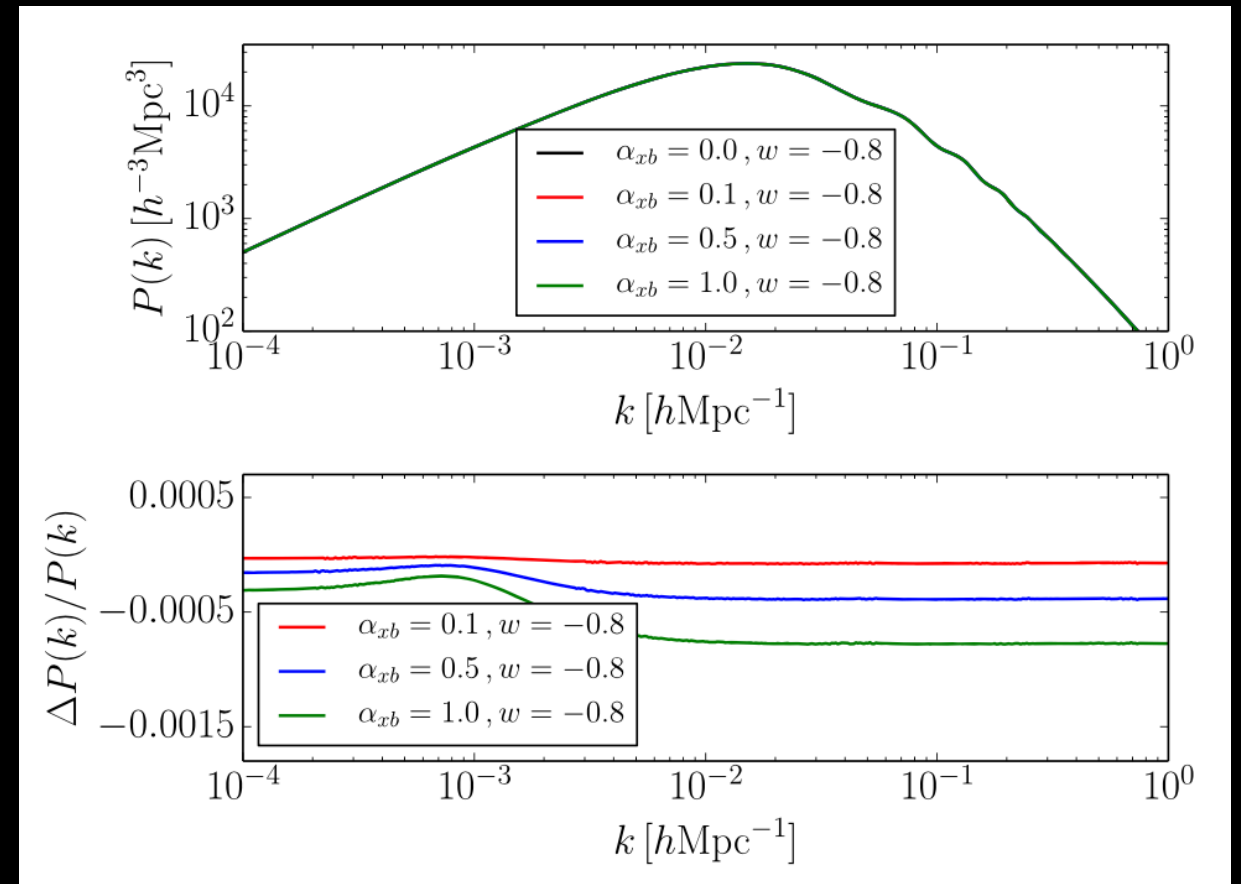
David Mota

Baryon - dark energy scattering

CMB temperature power spectrum



Matter power spectrum at $z = 0$



$$\alpha_{xb} = \sigma_{xb} / \sigma_T$$

Vagnozzi, LV+20

Reliable up to $k_{\text{max}} \approx 0.1 h\text{Mpc}^{-1}$

Baryon - dark energy scattering

What can we learn from collider searches?

DE is modeled as a scalar field ϕ of mass \ll SM

Possible scattering operators:

$$\mathcal{L}_1 = \frac{\partial_\mu \phi \partial^\mu \phi}{M_1^4} T^\nu{}_\nu \quad (\text{conformal}) \quad \longrightarrow \quad \sigma_1 \sim \frac{p_\phi^4 m_{\text{SM}}^2}{M_1^8}$$

$$\mathcal{L}_2 = \frac{\partial_\mu \phi \partial_\nu \phi}{M_2^4} T^{\mu\nu} \quad (\text{disformal}) \quad \longrightarrow \quad \sigma_2 \sim \frac{p_\phi^4 p_{\text{SM}}^2}{M_2^8}$$

$$M_1 \gtrsim 200 \text{ GeV}; \quad M_2 \gtrsim 1.2 \text{ TeV} \quad (\text{Brax+16; ATLAS19})$$

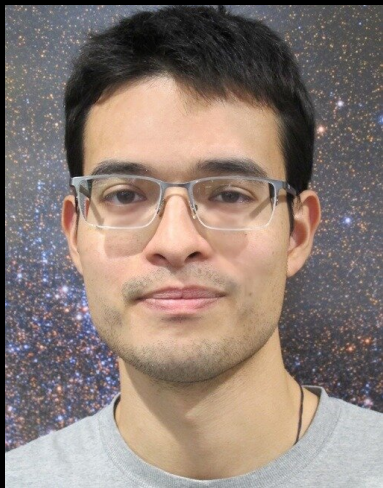
We generally expect $\alpha_{xb} \ll 1$

Baryon - dark energy scattering

Direct detection of dark energy: the XENON1T excess and future prospects

Sunny Vagnozzi,^{1,2,*} Luca Visinelli,^{3,4,†} Philippe Brax,^{5,‡} Anne-Christine Davis,^{6,1,§} and Jeremy Sakstein^{7,¶}

We explore the prospects for direct detection of dark energy by current and upcoming terrestrial dark matter direct detection experiments. If dark energy is driven by a new light degree of freedom coupled to matter and photons then dark energy quanta are predicted to be produced in the Sun. These quanta free-stream towards Earth where they can interact with Standard Model particles in the detection chambers of direct detection experiments, presenting the possibility that these experiments could be used to test dark energy. Screening mechanisms, which suppress fifth forces associated with new light particles, and are a necessary feature of many dark energy models, prevent production processes from occurring in the core of the Sun, and similarly, in the cores of red giant, horizontal branch, and white dwarf stars. Instead, the coupling of dark energy to photons leads to production in the strong magnetic field of the solar tachocline via a mechanism analogous to the Primakoff process. This then allows for detectable signals on Earth while evading the strong constraints that would typically result from stellar probes of new light particles. As an example, we examine whether the electron recoil excess recently reported by the XENON1T collaboration can be explained by chameleon-screened dark energy, and find that such a model is preferred over the background-only hypothesis at the 2.0σ level, in a large range of parameter space not excluded by stellar (or other) probes. This raises the tantalizing possibility that XENON1T may have achieved the first direct detection of dark energy. Finally, we study the prospects for confirming this scenario using planned future detectors such as XENONnT, PandaX-4T, and LUX-ZEPLIN.



Sunny Vagnozzi



Philippe Brax



Anne-C. Davis



Jeremy Sakstein

Baryon - dark energy scattering

Direct detection: chameleons

The chameleon is characterized by a density-dependent mass

$$m_\phi = m_\phi(\rho)$$

The mass results from the effective potential

$$V_{\text{eff}}(\phi) = V(\phi) + \rho \exp\left(\frac{\beta_m \phi}{M_{\text{Pl}}}\right)$$

$V(\phi)$ Bare potential

β_m Chameleon coupling with the species of density ρ

Chameleon production in the Sun

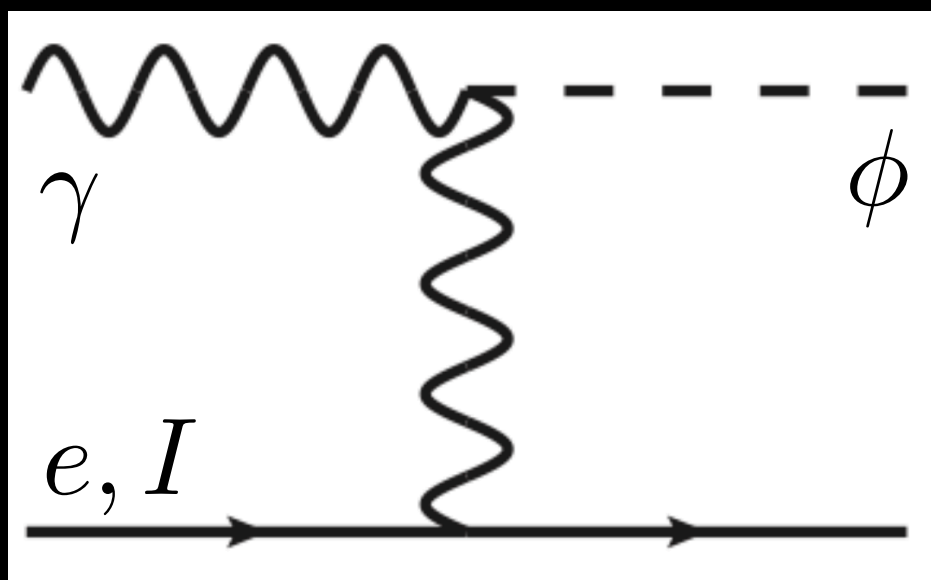
Chameleon production in the Sun differs from the axion case

$$S_{\phi\gamma} = \int d^4x \sqrt{-g} \left[-\frac{1}{4} F^{\mu\nu} F_{\mu\nu} - \beta_\gamma \frac{\phi}{M_{\text{Pl}}} F^{\mu\nu} F_{\mu\nu} + \frac{1}{M_\gamma^4} T_\gamma^{\mu\nu} \partial_\mu \phi \partial_\nu \phi \right]$$

(conformal) (disformal)

In practice, the disformal case is irrelevant in most of the space

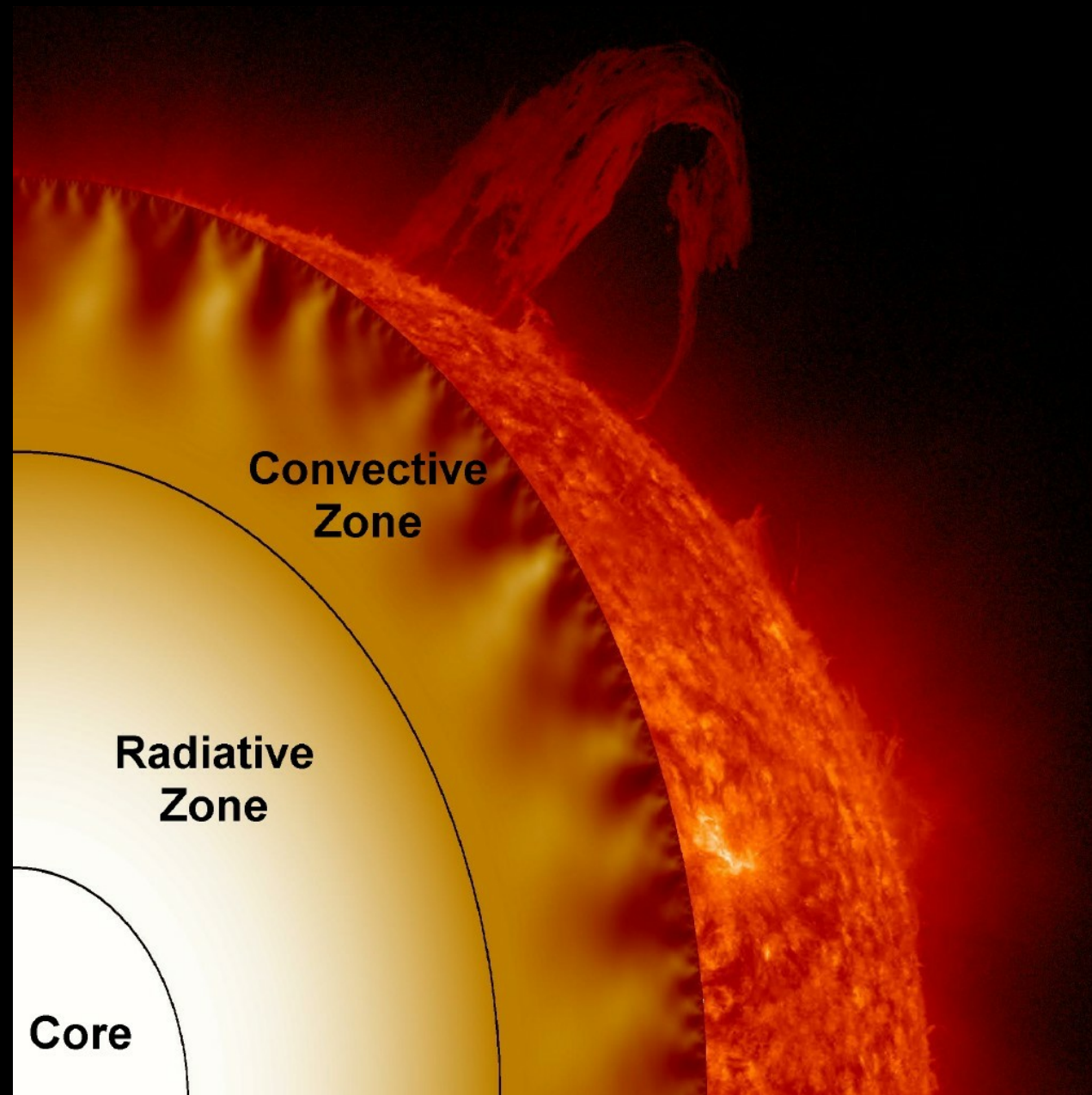
Production through Primakoff effect (Brax+11)



$$\frac{d\Phi_{\text{Earth}}}{d\omega} \propto \beta_\gamma^2 \omega^{3/2}$$

Vagnozzi, LV+21

Chameleon production in the Sun



Mostly occurs within a narrow region
at the Solar tachocline $R \sim 0.7R_{\odot}$

Detection of solar chameleons

Cross section $\sigma_{\phi e} = \sigma_{\phi e, \text{disf}} + \sigma_{\phi e, \text{conf}}$

The conformal coupling is negligible $\sigma_{\phi e, \text{conf}} \ll \sigma_{\phi e, \text{disf}}$

Disformal coupling $\mathcal{L} \supset \sqrt{-g} \frac{1}{M_e^4} \partial_\mu \phi \partial_\nu \phi T_e^{\mu\nu}$

Leads to the cross section $\sigma_{\phi e, \text{disf}} = \frac{m_e^2 \omega^4}{8\pi^2 M_e^8}$

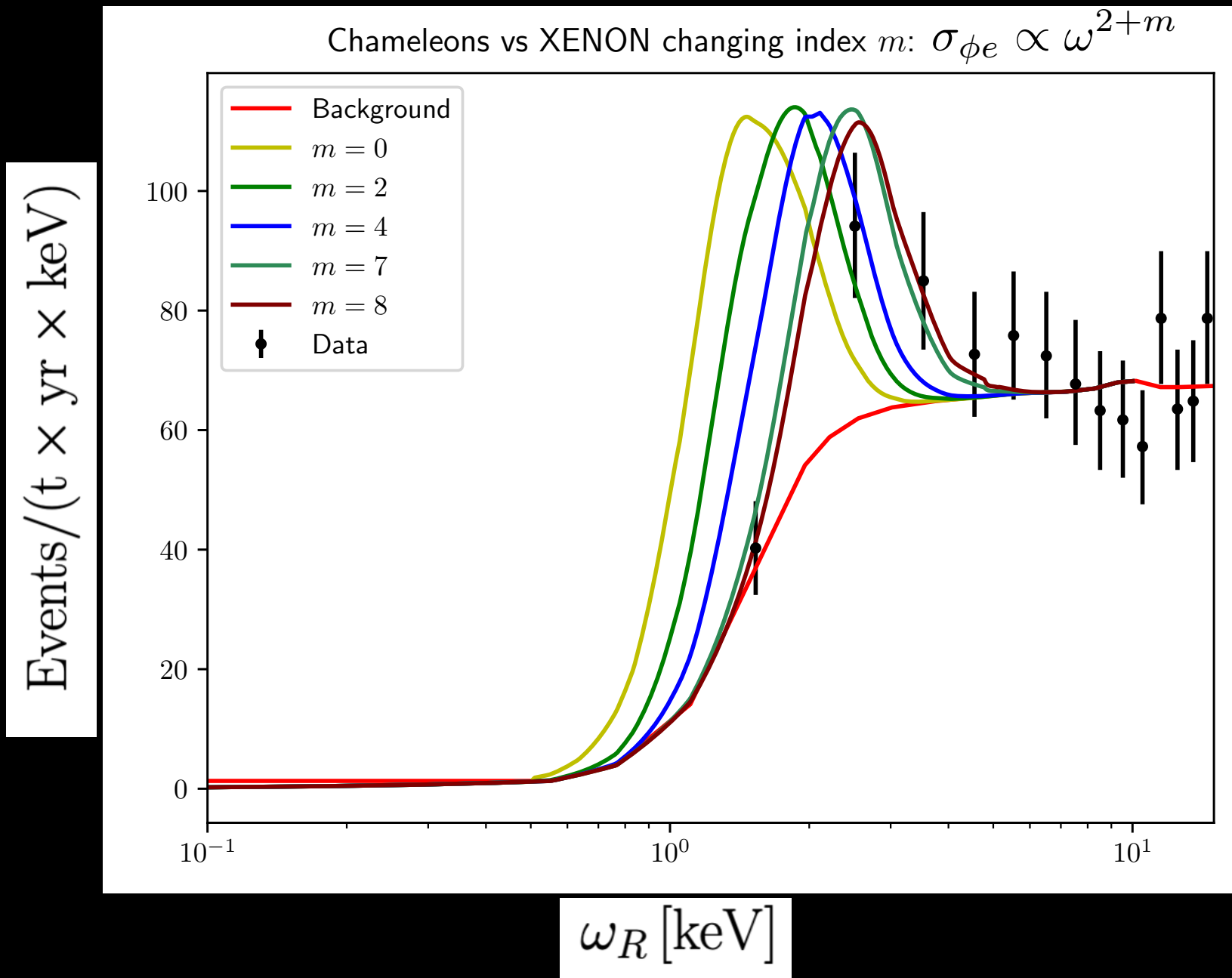
Vagnozzi, LV+21

Detection of solar chameleons

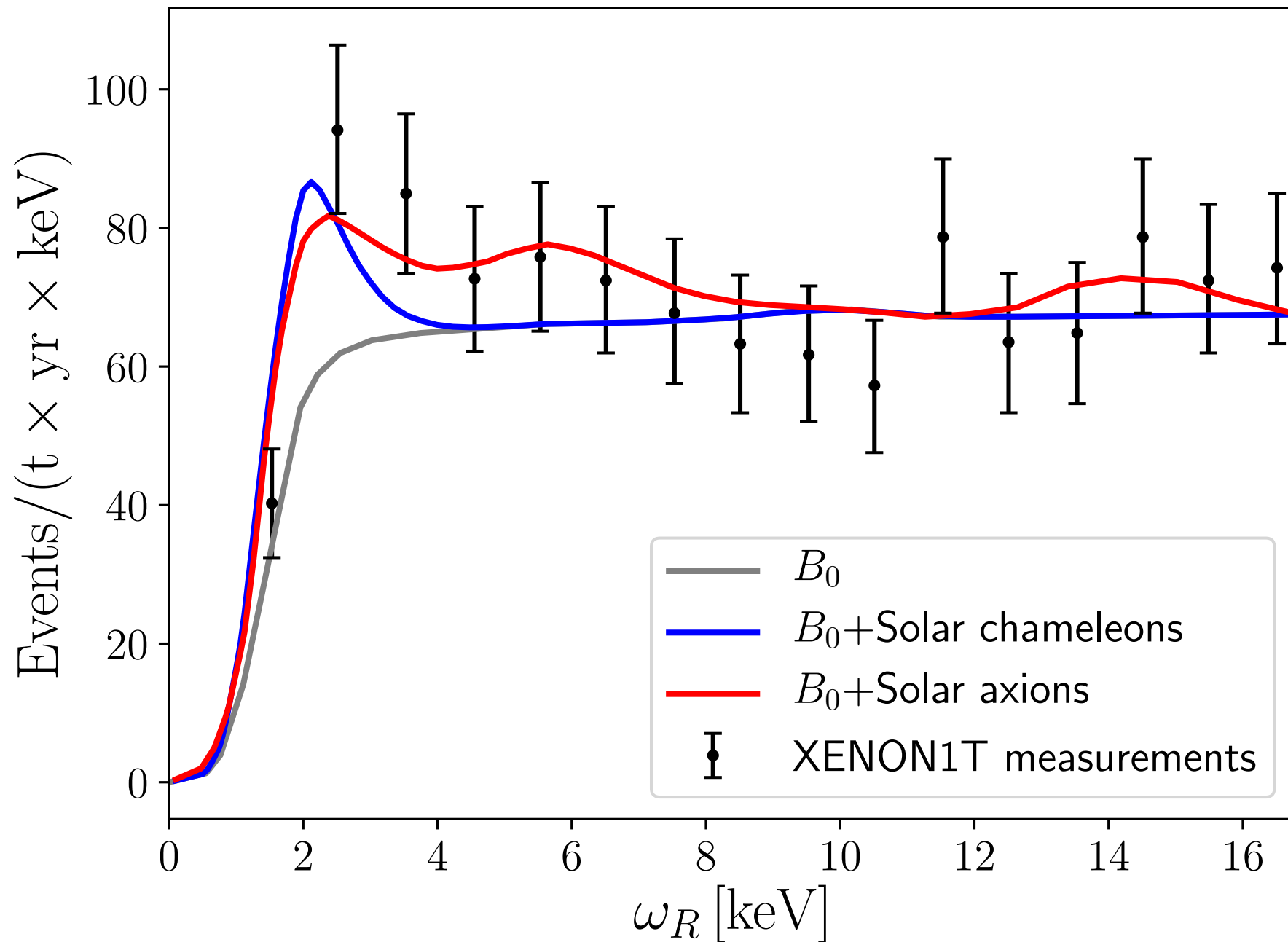
$$\frac{dR_0(\omega)}{d\omega} = N_{\text{Xe}} \frac{d\Phi_{\text{Earth}}}{d\omega} \sigma_{\phi e}$$

$m = 0$ (conformal)

$m = 2$ (disformal)



Detection of solar chameleons



Benchmark:

$$\beta_e = 10^2$$

$$M_e = 10^{3.7} \text{ keV}$$

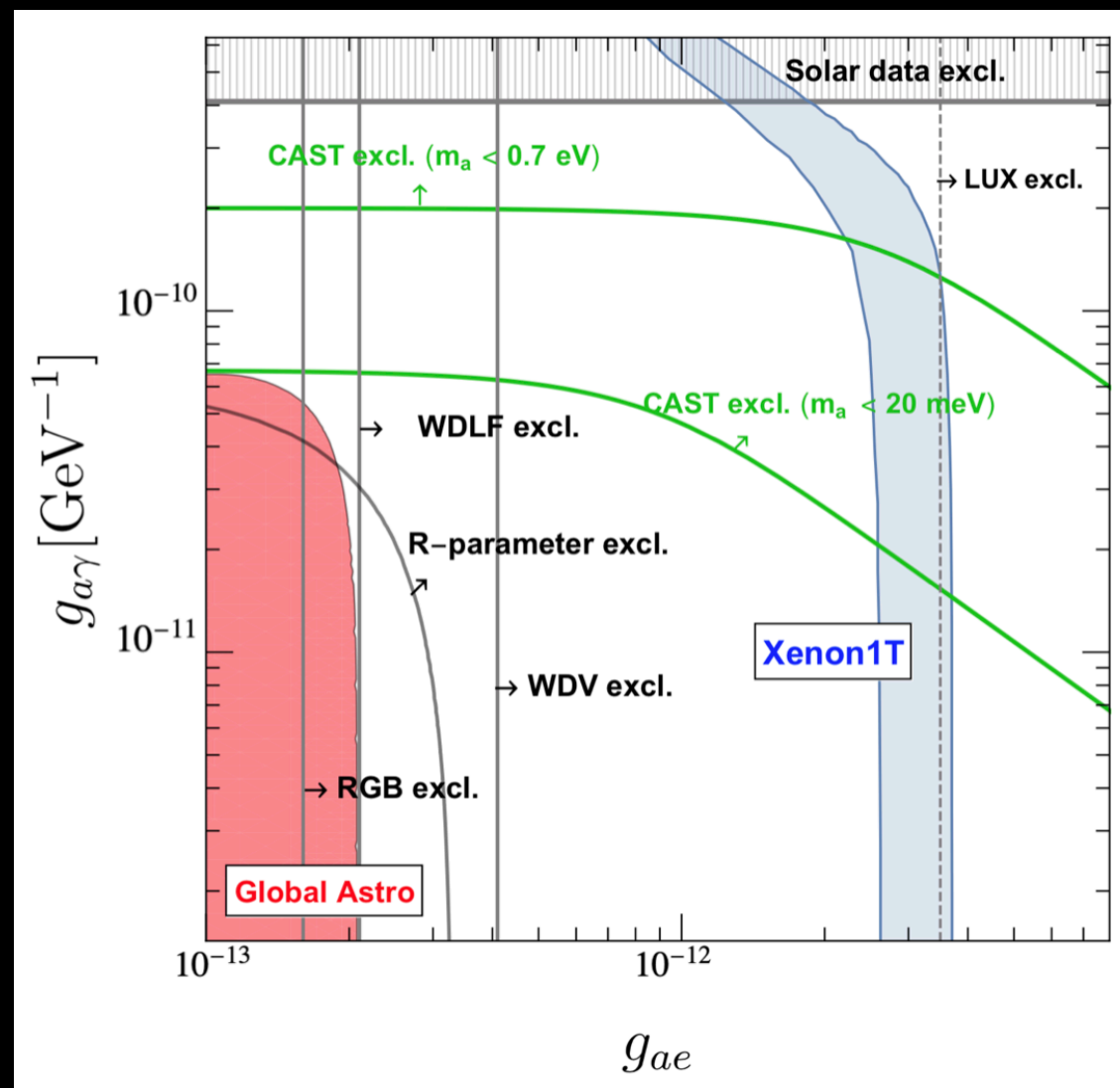
$$\beta_\gamma = 10^{10}$$

$$M_\gamma = 1000 \text{ TeV}$$

Vagnozzi, LV+21

Stellar bounds

The axion interpretation of the XENON1T excess is disfavored once the best-fit region is compared to what is expected from stellar production in RGB and white dwarfs



Chameleons are not affected by stellar cooling bounds because of the density-dependence of their mass: di Luzio+20

Chameleons are not produced in the cores of stars because of kinematic suppression $m_\phi \gg T_{\text{core}}$

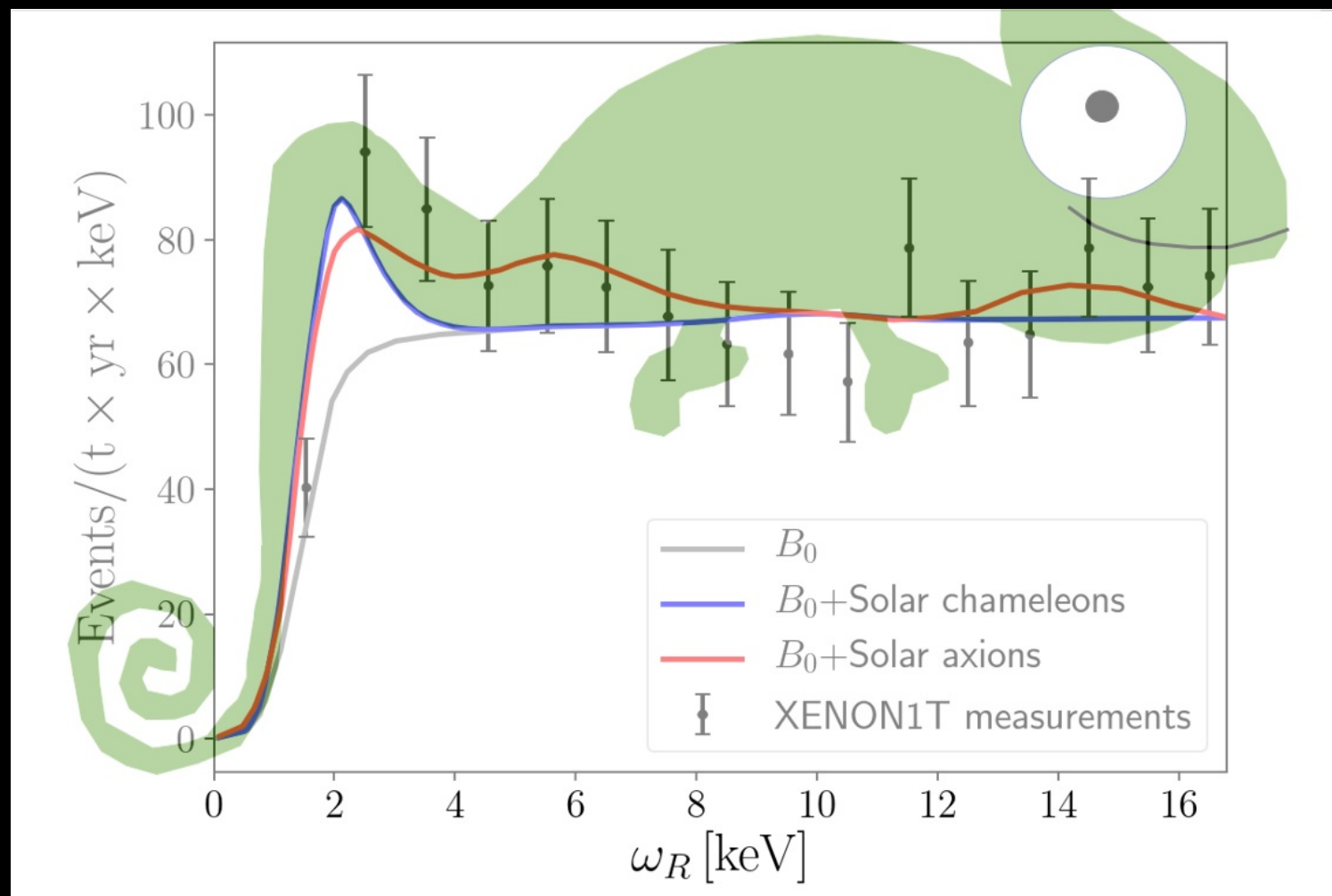
Experiment	Exposure (ton × yr)	Electron recoil background (ton × yr × keV) ⁻¹	Events / yr (expected)
XENON1T [72]	0.65	76.0	20
XENONnT [135]	20.0	12.3	180
PandaX-4T [134]	5.6	18.0	130
LUX-ZEPLIN [130]	15.0	14.0	250

TABLE I. Expected exposure in units of ton × yr (tonne-year) and electron recoil background in units of (ton × yr × keV)⁻¹ for recoil energies $\lesssim 10$ keV, expected for the upcoming XENONnT [135], PandaX-4T [134], and LUX-ZEPLIN [130] experiments, which will be able to confirm or disprove the XENON1T excess. The last column reports the number of excess events that are expected per year in each detector, in the energy range (1 – 30) keV.

Conclusions

The dark energy section can be probed in the future by:

- Cosmological probes
- Collider searches
- Direct detection experiments



The chameleon model could already be accessible in the next generation of DD searches

Its unique features could lead to an identification using complementary searches (ADMX)